Multimodel Approach to Personalized Autonomous Adaptive Cruise Control

Andrew Phillip Bolduc ¹⁰, Longxiang Guo, and Yunyi Jia ¹⁰, Member, IEEE

Abstract—Autonomous vehicles are gaining increased attention but surveys have shown that a large percentage of people are wary of adopting the new technology. One possible explanation for the hesitancy is that the occupant would not be comfortable with the driving style as a result of the control models and their parameters as set by the manufacture. Comfort level is subjective in nature and therefore varies between individuals. To combat this issue, autonomous vehicles must be able to adapt to the driving style preference of the user. If we assume drivers are more comfortable with their own driving style, we can choose to have the vehicle learn and incorporate the driver's style into the control models. However, there is still no widely accepted "best" model. One model may prove to better represent a particular driver than other models though a driver may choose unsafe driving conditions, the replication of which should not take precedence over the safety of the occupant. In this paper, we propose a multimodel approach to find the best driver model for describing an individual's longitudinal driving style on highway. A method for extracting the indicators of an individual's driving style is proposed first. Then, a multimodel-based evaluation method is described in detail. Chandler, Herman, & Montroll, General Motors Nonlinear, Tampère, Addison & Low, Optimal Velocity Model, and Neural Network models are trained and compared in this paper. The model with the best performance in replicating driving style is further coupled with a model predictive controller to include safety constraints for safer driving. Finally, the proposed multimodel approach is tested with driving data collected from five different drivers. The test results show that our multimodel-based approach is showing advantage over a single model approach in imitating an individual's longitudinal driving style.

Index Terms—Autonomous vehicles, driver modeling, adaptive cruise control, model predictive control.

I. INTRODUCTION

MAJOR reason for studying longitudinal driving behavior of drivers is to aid in the development autonomous driving systems such as adaptive cruise control [2]. Because drivers are skeptical of autonomous vehicles taking over the vehicle control task [3], [4], drivers need to be comfortable with the driving style produced by the Adaptive Cruise Control (ACC) system. A survey conducted by the American Automobile Association (AAA) found that 75% of the 1,832 respondents are afraid to ride in an

Manuscript received November 22, 2017; revised February 22, 2018 and December 12, 2018; accepted January 3, 2019. Date of publication April 26, 2019; date of current version May 22, 2019. This work was supported by the National Science Foundation under Grant CNS-1755771. (Corresponding author: Yunyi Jia.)

The authors are with the Department of Automotive Engineering, Clemson University, Clemson, SC 29634 USA (e-mail: abolduc@g.clemson.edu; longxig@g.clemson.edu; yunyij@clemson.edu).

Color versions of one or more of the figures in this paper are available online at http://ieeexplore.ieee.org.

Digital Object Identifier 10.1109/TIV.2019.2904419

autonomous vehicle with 84% who do not want an autonomous vehicle trust their skills more than the vehicle [3]. Similarly, reference [4] found that 66.8% of 1,533 respondents were moderately to very concerned autonomous vehicles would not drive as well as humans. People are having those feelings because of two major concerns, the first is that the autonomous vehicle may not actually drive safely in terms of technical standards; the second is while the vehicle is technically driving safely, the passenger may not have a safe feeling since the autonomous driving style is different from the human's driving style. To help alleviate the second concern, thorough insights into human driving behavior are needed to ensure the autonomous control is able to reproduce the driving style the driver is accustomed.

A. Related Work

ACC differs from conventional cruise control systems by continual adjustment of the vehicle speed in response to a change in distance to the vehicle in front. Many studies have investigated mathematical models that mimic human drivers to provide a more personalized ACC [2], [5], [6]. These ACC controllers typically are designed to represent an average human driving style and certainly do not reflect individual driving preference. There has been increasing research to study how to better represent the individual driving style mostly through use of machine learning methods [7]–[11].

Vaitkus *et al.* [7] propose a k-nearest neighbors (KNN) based method for classifying driving styles into aggressive or normal by using acceleration information. This method is showing its effectiveness on the same route. However, although using only acceleration information can be effective on a fixed route, it will not work under real driving scenario. Moreover, classification is not enough for mimicking an individual's unique driving style.

Nvidia [8] proposes an NN based end-to-end learning method for autonomous driving. The CNN architecture in this literature is very effective in adapting to different driving styles, but since it is an end-to-end method, a huge amount of training data is required to train the NN as compared to traditional, model-based methods. Once it is trained to one style, it is extremely difficult to tailor it to fit other driving styles, which makes it almost impossible to be applied to different drivers. Kuderer *et al.* [9] propose an inverse reinforcement learning (IRL) method to learn individual driving styles using extracted features. Like the NN based end-to-end learning method, this method is effective when the amount of training data is large, but is difficult to be transferred to a different driver. Macadam *et al.* [10] propose an NN

2379-8858 © 2019 IEEE. Personal use is permitted, but republication/redistribution requires IEEE permission. See http://www.ieee.org/publications_standards/publications/rights/index.html for more information.

based architecture for identifying driving style and classifying headway control behaviors of individual drivers. Compared to the method in [8] and [9], it does not require as much data to train the NN since it is a classification application, but it is not able to produce continuous vehicle control command, thus not suitable for being used as vehicle controller directly.

In [11] a fuzzy logic neural net was constructed for carfollowing and safety-critical events using "naturalistic" driving data. The authors proposed a model that behaves like one driver under certain events and like another under other events. The concept is for the controller to behave like the individual driver unless a safety-critical scenario unfolds, under which the safer driver model takes control. However, this blending of driving models still relies on having multiple models derived from data which at least one must be assumed to be safe under many possible events. There is no guarantee that either model properly handles safety-critical events appropriately.

Lefèvre, Carvalho, and Borrelli [12] used a learning by demonstration approach to generate a driver model from real driving data. Their singular model was a combination of Hidden Markov Model and Gaussian Mixture Regression with an output of desired acceleration given as a reference for an MPC controller to impose constrains to actuators, speed, and following distance while minimizing jerk. However, their evaluation procedure was limited to inverse Time-To-Collision (TTCi) and Vehicle Specific Power (VSP), the instantaneous engine load of the vehicle [13], as driving style indicators.

Many other mathematical models have been offered over the past decades to quantitatively describe driver behavior with varying success [14]. However, no one model is widely accepted as the best at replicating individual driver behavior [15]. This may be due to one model being able to represent an individual driver while another better representing a different driver. Additionally, driver representation may not necessarily mean producing the identical control response, but rather, reproducing the driving style (i.e., desired following distance, approaching behavior, preferred acceleration levels, etc.) [16]. Furthermore, the control output of the driver model does not guarantee safe operation.

MPC has long been used over other conventional techniques for complex dynamical systems due to the inherent ability to predict future conditions and apply preemptive control while remaining within desired constraints. Many studies have explored the use of MPC for adaptive cruise control and demonstrated its ability to handle conditions not accounted for in the reference control model [17]–[21].

B. Contribution

In this paper, we list key driving style indicators and propose a method of indicator extraction from driving data that can be obtained from sensors commonly used in vehicles equipped with ACC. We then propose an adaptive multi-model approach that utilizes this data to adapt control model parameters of multiple models and to train a neural network. Each model is validated through car-following simulation over highway speeds and the driving style indicators of each model are compared to those of the driver. We believe reproducing driving style indicators

is more representative of the driver's desired behavior, on average, rather than mimicking the driver's acceleration at each time instant. Finally, Model Predictive Control is constructed and simulated to track the reference trajectory of the model that best represents the driver's style. Safety constraints are imposed on our MPC to handle situations where the driver model would fail to prevent occupant harm. A short comparison of the MPC and the driver model performance is discussed.

Therefore, the major contributions of the paper can be summarized as:

- Propose and validate an approach to characterize the individual's ACC driving style by defining and extracting measurable parameters.
- Propose and validate a multi-model approach to synthesize the best ACC driver model to replicate an individual's driving style.
- Propose and validate an approach to execute the best driver model to achieve personalized adaptive cruise control driving by using model predictive control and imposing safety constraints onto the best model which is unable to handle safety concerns alone.

This paper is arranged in the following manner. Driving style indicators and safety criteria are defined in Section II. Section III describes the method for extracting the style indicator from human driving data. The framework for the proposed multi-model approach is given in Section IV. The controller for implementing the driver model is presented in Section V. Experimental results are shown in Section VI and the paper concludes with Section VII.

II. DRIVING STYLE AND SAFETY

A. Style

The car-following scenario includes a lead vehicle and at least one following vehicle traveling in the same lane. The driver of the following car applies acceleration or deceleration to maintain a preferred distance and keep pace. During these conditions, identifiable habits can be observed. Driving style indicators are these measurable habits the individual driver exhibits in the operation of the vehicle and reveal how the driver drives on average and how that operation fluctuates [16]. Style indicators can also be extracted from a driver model and used to determine how well the model represents the style an individual driver. In this study, we focus solely on indicators of longitudinal driving style which are summarized in the Table I.

B. Safety

Regarding longitudinal safety parameters, two main safety criteria often appear in literature and are commonly used in driver assistance functions, time headway (THW) and time to collision (TTC). In this paper, we apply these metrics to determine whether the driver or controller behavior is unsafe. Too short of a time headway when following a vehicle, known as tailgating, is a leading cause of rear-end crashes [22]. The National Highway Traffic Safety Administration (NHTSA) found that rear-end crashes ranked the highest (~2.1 million cases or

| TABLE I |
|---------------------------|
| DRIVING STVI E INDICATORS |

| Symbol | Quantity | Definition |
|----------|---|------------------------|
| a_p | mean of maximum accelerations | preferred acceleration |
| b_p | during accelerator operation mean of maximum decelerations during brake operation | preferred deceleration |
| THW_p | mean of mean time headway ^a | preferred time headway |
| | during steady vehicle following events | |
| THW_f | standard deviation of mean time | time headway |
| | headwaya during steady following | fluctuation |
| TIII | events mean of standard deviation of time | fallossina atahilits |
| THW_s | | following stability |
| | headway ^a during steady following events | |
| $TTCi_d$ | mean of maximum inverse time to | preferred maximum |
| | collision ^b while approaching | danger level |
| $TTCi_f$ | mean of minimum inverse time to | preferred maximum |
| | collision ^b while falling behind | falling behind level |

^aTime headway refers to the time it takes the following vehicle to reach the same point as the lead vehicle given the current speeds of both vehicles and distance between the front of both vehicles. For reasons of having an unknown vehicle length and for simplicity, the length of the predecessor's vehicle is taken as zero in this paper. ^bTime to collision refers to the time it takes for the following vehicle to collide into the lead vehicle given the current relative speed and distance

33.4%) in police-reported automobile accidents in the US in 2015. These accidents resulted in more than 2,200 fatalities and approximately 500,000 injuries [23]. Tailgating is the major contributing cause for rear-end crashes with a deadly consequence [22]. Drivers regularly tailgate by maintaining headways of one second or less [24], however, driver training programs in the US recommend THW should follow the 2-second rule to remain outside the tailgating region.

A TTC threshold of 4 seconds (TCCi of 0.25 s⁻¹) is usually chosen for safety braking systems and has been used to differentiate between cases where the driver is in a dangerous state from cases where the driver is in control [25]. In [26], a minimum TTC value, where safety is a concern, of 3.5 s was determined for the non-supported drivers, and 2.6 s for supported drivers.

III. DRIVER CHARACTERIZATION

The proposed method of determining style indicators requires collecting pedal operation, vehicle speed and acceleration, and inter-vehicle distance and speed.

During periods of accelerator and brake operation, the maximum value is recorded. The maximums of all segments are averaged and are considered as preferred acceleration and deceleration levels of the driver. Acceleration values for Driver 1 through 3 are shown as examples in Fig. 1 with points indicating maximum acceleration and deceleration for each segment of pedal operation. The dashed line represents mean at approximately .5, 1.2, and .4 m/s² for preferred acceleration and -1.6, -2.2, and -2.2 m/s² for preferred braking level for Drivers 1, 2, and 3, respective. Fluctuation in acceleration is minor for Drivers 1 and 3 but is most prominent in the results for Driver 2. The high variance can be explained by driver inattention or poor motion cuing in the simulation. It is worth reiterating that

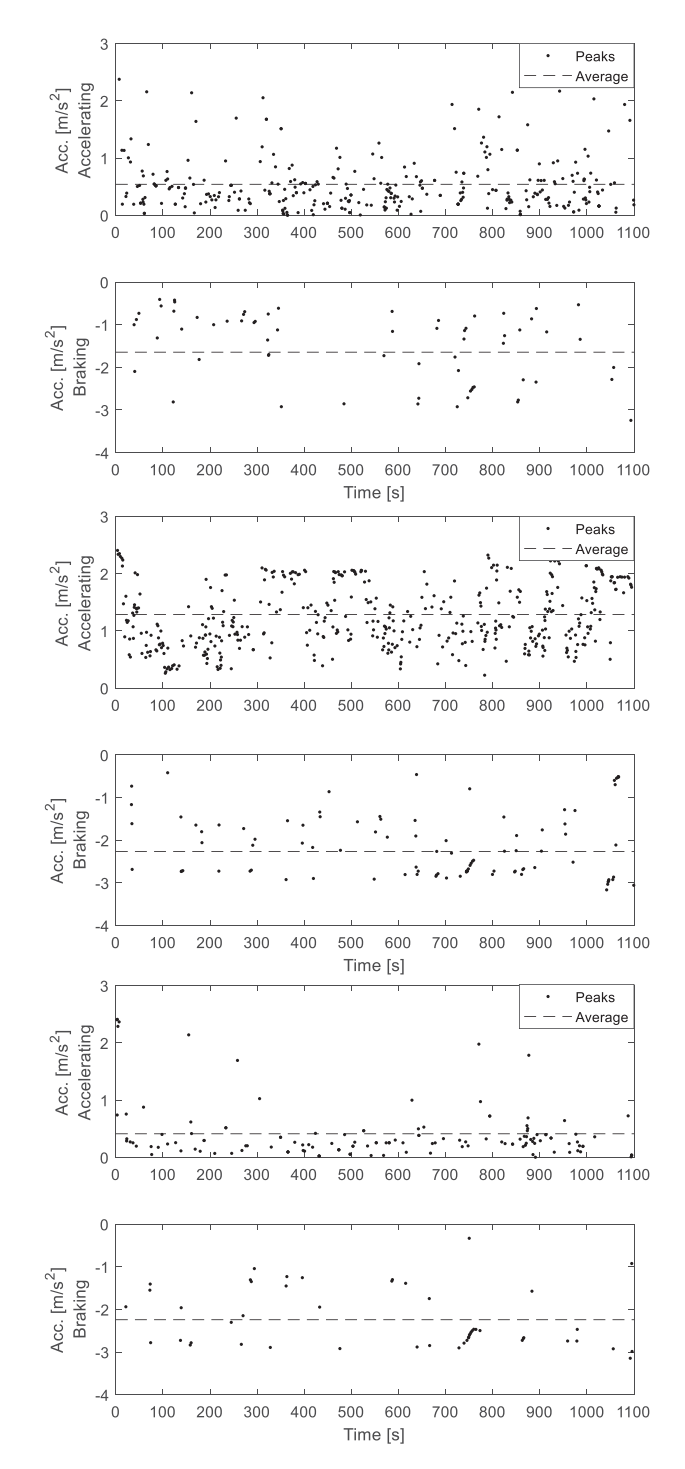


Fig. 1. Maximum acceleration and deceleration for each period of pedal operation for Driver 1 through 3, in descending order. Mean shown with dashed line.

the driver's desired acceleration lies in the average of his or her peak accelerations.

The steady following condition occurs when THW is below 6 seconds [27] and TTCi is below $0.05 \, \mathrm{s}^{-1}$ for 5 seconds or more [16]. During each segment of steady following, the average time headway is recorded as the desired THW. The average of all the segment averages is taken as preferred time headway and the standard deviation of all the segment averages gives THW

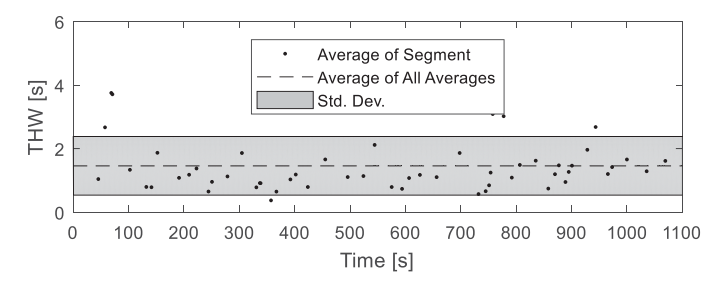


Fig. 2. Mean THW of each steady following segment, preferred THW, and THW fluctuation for Driver 1.

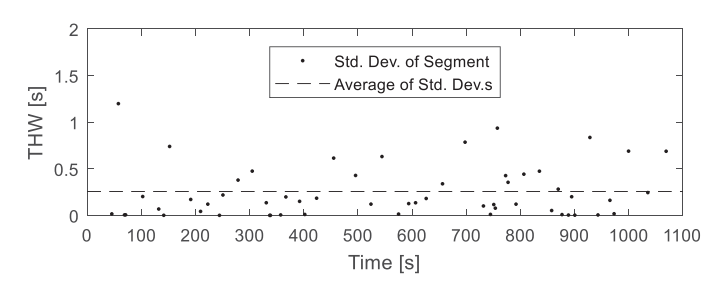


Fig. 3. THW fluctuation represented by Average of Std. Dev.s for Driver 1.

fluctuation level. THW Indicators for Driver 1 are represented in Fig. 2 with the average of each segment illustrated by points, preferred THW shown by a dashed line, and THW fluctuation by the shaded grey area.

The driver's following stability is determined by calculating the standard deviation in each steady following segment and taking an average of all the standard deviations (THW_s) . Driver 1 has scored 0.237 in THW_s as shown in Fig. 3 with points representing the standard deviation of each following segment and the mean shown with a dashed line. Driver 2 and 3 has 0.604 and 0.128 in THW_s respectively. When combined with Fig. 1, it can be seen that driver 2 has the least following stability and is having scattered acceleration, thus his THW_s value is the highest among these 3 drivers. Driver 3 is a stable driver during most of the time. Although he has made a few large accelerations, he still has the lowest THW_s value.

In data segments when the driver is approaching the lead vehicle (positive segments of TTCi), the maximum value is recorded. The average of all the maximum values gives driver's preferred danger level when approaching. Similarly, the average of all the minimums in negative segments of TTCi givers driver's preferred falling behind level. Preferred TTCi for Driver 1 is shown in Fig. 4 where maximum and minimum are represented with points and the preferred level with dashed lines.

IV. MULTI-MODEL APPROACH

A. Framework

Our multi-model framework for adaptive cruise control includes multiple model parameter fitting using driving data generated by a human driver, driver and driver model style identification and comparison to provide a control reference that the driver recognizes as familiar, and model execution by MPC

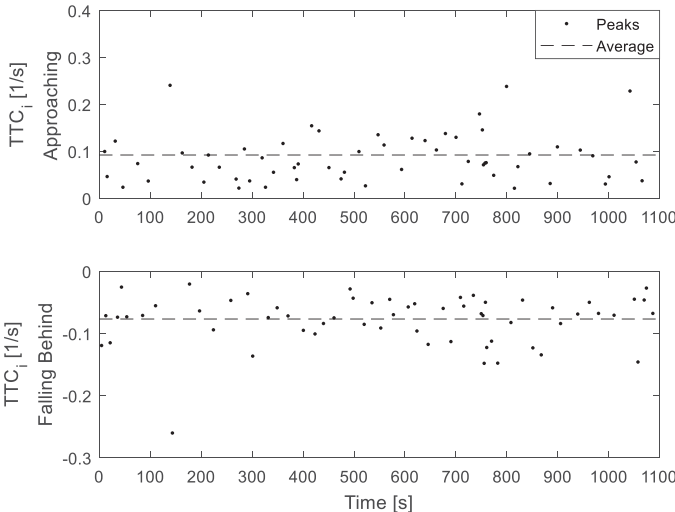


Fig. 4. Mean maximum and minimum TTCi levels. Preferred approaching danger and falling behind levels.

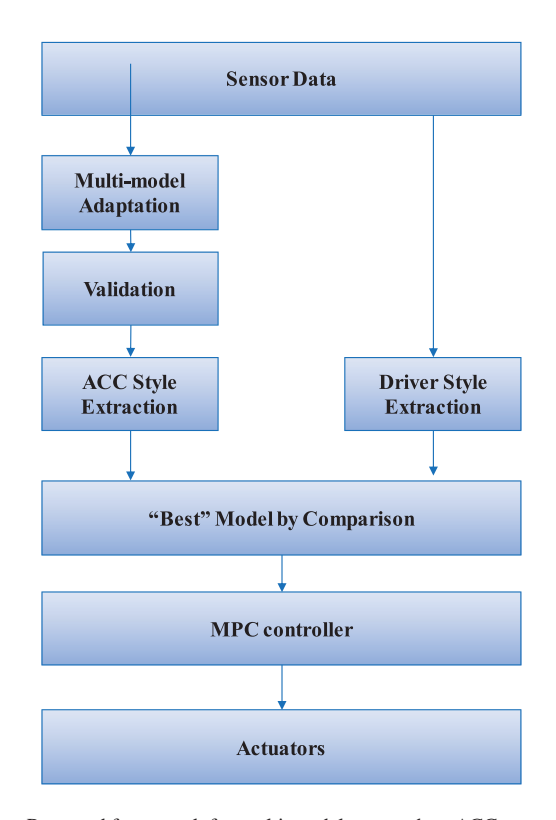


Fig. 5. Proposed framework for multi-model approach to ACC.

which uses model predictions to provide control. The proposed framework is illustrated in Fig. 5 and is described from top down below.

- For the car-following scenario, sensor data includes following vehicle acceleration, speed, inter-vehicle speed and distance which can be collected via on-board sensors commonly available on vehicles equipped with ACC.
- In the multi-model adaption phase, sensor data is used to fit control model parameters, train a neural network, etc. for

the purpose of mimicking the driver's style. Each model is validated through simulation over further driving data.

- The ACC and driver style extraction computes the indicators from the validation phase and compared to another by absolute relative error between indicators.
- The driver model that best replicates the style of the driver is used as a reference for a MPC controller with safety constraints added. The MPC is then deployed to control the vehicle.

B. Driver Models

There have been multiple attempts to model the longitudinal behavior of the human driver. The authors intend to evaluate multiple such models that have been selected based on a review of the most commonly accepted. These models include Chandler, Herman, & Montroll (CHM) [1], General Motors Nonlinear (GM) [28], Tampère (TMP) [29], Addison & Low (AL) [30], and the Optimal Velocity Model (OVM) [31]. Each of these models assumes the driver is able to perceive relative speed and distance between their vehicle and the vehicle which they follow and react by applying braking or acceleration.

CHM and GM driver models both assume the driver reacts to a change in relative velocity. CHM takes the form

$$a^f(t+\tau) = c_1^* \Delta v(t) \tag{1}$$

where

$$\Delta v(t) = \left(v^l(t) - v^f(t)\right) \tag{2}$$

 $a^f(t+\tau)$ and $v^f(t)$ is the acceleration and velocity of the following vehicle and $v^l(t)$ is the velocity of the lead vehicle. t is the current moment in time and τ is time is takes the driver to accelerate after a change in stimulus, or reaction time. c_n is the sensitivity constant.

GM adds an additional sensitivity term $1/\Delta d(t)$ where $\Delta d(t)$ is the inter-vehicle distance. The sensitivity term increases the magnitude of response as inter-vehicle distance decreases.

$$a^{f}(t+\tau) = c_{2}^{*} \frac{1}{\Delta d(t)} \Delta v(t)$$
(3)

CHM and GM have been shown to mimic velocity tracking behavior with moderate success however neither account for the driver's behavior in maintaining a desired headway distance. Both allow the following vehicle to follow arbitrarily close to lead vehicle when velocities are matched. TMP and AL add an additional term in an attempt to model distance tracking. The TMP model is given by

$$a^{f}(t+\tau) = c_{3}^{*} \Delta v(t) + c_{4}^{*} \left(\Delta d(t) - d^{d}(t) \right)$$
 (4)

Here d_t^d is the desired distance of the driver at a given speed.

$$d^{d}\left(t\right) = d_{0} + \lambda v^{f}\left(t\right) \tag{5}$$

where d_0 is the minimum distance. AL adds the sensitivity term and distance tracking becomes a cubic function.

$$a^{f}(t+\tau) = c_{5}^{*} \frac{1}{\Delta d(t)} \Delta v(t) + c_{6}^{*} (\Delta x(t) - d^{d}(t))^{3}$$
 (6)

The OVM model was proposed in [31] and states that the driver chooses an optimal velocity based on the current following distance and adjusts his or her speed. The model is given by the following equations

$$a^{f}\left(t+\tau\right) = c_{7}^{*}\left(V^{opt}\left(\Delta d\left(t\right)\right) - v^{f}\left(t\right)\right) \tag{7}$$

 $V^{opt}(\Delta d(t))$ is the optimal velocity function of the following distance which was proposed in [32] and is determined by the monotonically increasing exponential function

$$V^{opt}\left(\Delta d\left(t\right)\right) = V_{\text{max}} \cdot \left[1 - e^{-\alpha(\Delta d\left(t\right) - d_0)}\right] \tag{8}$$

where α and slope of the exponential function and $V_{\rm max}$ is the maximum velocity of the following vehicle [33], [34].

Lastly, we train a neural network for each driver with the available kinematic states from simulated car-following trials using MATLAB Neural Network toolbox. This toolbox uses a two-layer feed-forward network with sigmoid hidden neuron and linear output neurons and is trained using Levenberg-Marquardt optimization algorithm with Bayesian regularization backpropagation, to prevent overfitting. Bayesian regularization was chosen due to its good generalization qualities for small, noisy datasets [35], [36]. Input for this neural network consists of following vehicle speed and inter-vehicle distance and speed data. As in the case of the previous driver models, driver acceleration was chosen as output.

V. Personalized Control Execution

MPC solves a constrained finite-time optimal control problem at each sampling instance which gives a sequence of control inputs, the first of which is applied to the system. At the next sampling instance, new measurements are taken and the computation repeats itself.

After the best model has been determined, the model output acceleration generates a velocity at each time step, using a point-mass vehicle model, as reference for our MPC whose goal is to follow this reference. Additionally, limits to controller output and safety level are added to prevent dangerous conditions, such as a rear-end collision or loss of vehicle stability, from arising. The MPC assumes the lead vehicle maintains constant speed and acceleration and the prediction of the following vehicle positions and velocities formulate constraints on THW, TTC, and minimum distance. Our MPC solves the constrained optimization problem over a prediction horizon and gives a sequence of torque, which ultimately results in acceleration. A similar framework for our MPC is described in detail in [25] and [26].

A. Vehicle Model

To update the states, the MPC uses a point-mass kinematic model for the following vehicle specified by the following equations

$$d(t + k + 1|t) = d(t + k|t) + v^{f}(t + k|t) \cdot \Delta t_{d} + \frac{1}{2}a^{f}(t + k|t) \cdot \Delta t_{d}^{2}$$
(9)

$$v^{f}(t+k+1|t) = v^{f}(t+k|t) + a^{f}(t+k|t) \cdot \Delta t_{d}$$
 (10)

where x(t+k+1|t) denotes the expected value of x(t+k) with available information at instant t, and Δt_d is the time in discretized form. The lead vehicle's future behavior cannot be determined; therefore, its states are assumed not to change.

B. Propagation Model

As in the vehicle model, the propagation model also includes a kinematic point mass model. The driver model provides the controller with a reference velocity computed using past driving states and output acceleration from the selected driver model, which is assumed constant. The propagation model assumes the lead vehicle does not change velocity.

$$v^{ref}\left(t\right) = v^{ref}\left(t-1\right) + a^{ref}\left(t-1\right) \cdot \Delta t_{d} \quad (11)$$

$$\Delta d(t+1) = \Delta d(t) + \Delta v(t) \cdot \Delta t_d - \frac{1}{2} a^f(t) \cdot \Delta t_d^2 \quad (12)$$

$$\Delta v(t+1) = \Delta v(t) - a^f(t) \cdot \Delta t_d \quad (13)$$

$$v^{f}(t+1) = v^{f}(t) + a^{f}(t) \cdot \Delta t_{d}$$
 (14)

where $v^{ref}(t)$ is the reference velocity of the following vehicle the controller tracks and is calculated from the driver model generated acceleration $a^{ref}(t-1)$ at the previous time step.

C. MPC Implementation

The controller seeks to minimize the cost function within safety constraints.

$$\min_{a_t} \sum_{k=0}^{N_c - 1} \left[v^f(t+k|t) - v^{ref}(t+k) \right]^2$$
 (15)

s.t.

$$T_{min} < T(t + k + 1|t) < T_{max}$$
 (16)

$$THW_{min} \le THW(t+k+1|t) \tag{17}$$

$$TTC_{min} \le TTC(t+k+1|t) \tag{18}$$

$$0 \le v^f(t+k+1|t) \tag{19}$$

$$d_{min} \le \Delta d(t + k + 1|t) \tag{20}$$

where N_c is the predicted horizon and T_{min} and T_{max} are the torque limits at the wheel for braking and acceleration. THW_{min} is the minimum time headway (1 sec.) to prevent tailgating and TTC_{min} is the minimum time to collision (4 sec.) to prevent a dangerous approaching conditions. Additionally, the controlled vehicle is not allowed to reverse and must not exceed a minimum following distance (d_{min}) of 10 meters.

In the simulator, the driver's chosen following distance may be shorter than what may be seen real-world driving, especially at higher speeds. This phenomenon can be explained by the overestimation of distance in the simulator and the lack of motion cuing, life-threatening risk, and full dynamics of the simulated vehicle in the simulator as compared to the real world [38], [39]. Therefore, we arbitrarily chose a shorter "safe" THW of 1 second to better represent the driver intentions.



Fig. 6. View of the driver participant in the simulator.

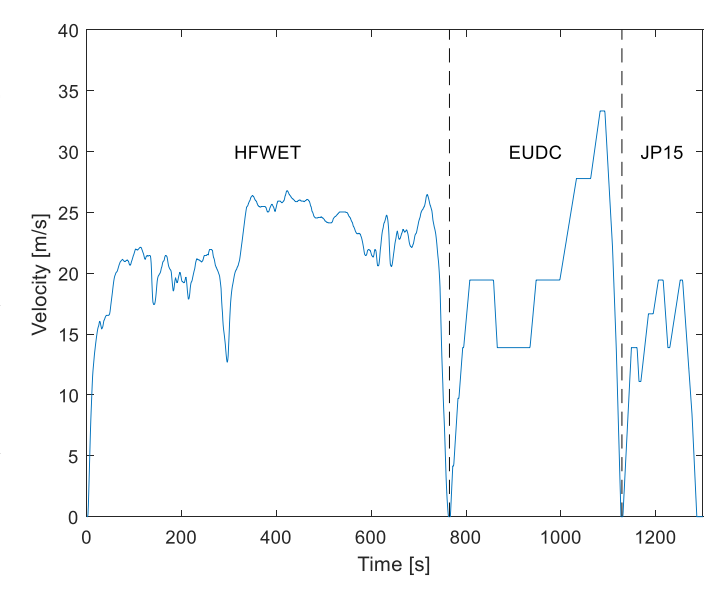


Fig. 7. Velocity profile of lead vehicle.

VI. EXPERIMENTAL RESULTS

A 3D environment was constructed in Simulink and included two vehicles, one automated leader car and one controlled by the human subject. Vehicle models were built with longitudinal dynamics and the human subject had real-time control of the following car via throttle and brake to simulate realistic conditions. The driver's view is shown in Fig. 6.

Participants were asked to follow a lead vehicle whose velocity profile was a combination of two commonly used drive cycles, HWFET, EUDC, and JP15 Mode. The HWFET and JP15 cycles are commonly used for emissions tests and represent a realistic highway driving scenario. For the latter reason, these two cycles were used for driver identification and control model construction. The EUDC cycle was chosen for model verification as it includes a wide range of speeds, including at magnitudes greater than those seen in other two. Lead vehicle velocity profile for the combined cycles is shown in Fig. 7.

Driver data was collected from five participants who had control of the throttle and brake of a following vehicle. The derived indicators of each trial, seen in Table II, show Driver 3 was the most relatively aggressive in terms of preferred acceleration and

TABLE II
DERIVED DRIVING STYLE INDICATORS FOR PARTICIPANTS

| Indicator | Driver 1 | Driver 2 | Driver 3 | Driver 4 | Driver 5 |
|------------------------------|----------|----------|----------|----------|----------|
| $a_p \text{ (m/s}^2\text{)}$ | 0.520 | 0.563 | 1.228 | 0.351 | 0.396 |
| $b_p (\text{m/s}^2)$ | -1.530 | -2.026 | -2.201 | -1.714 | -2.233 |
| THW_p (s) | 1.357 | 3.197 | 1.290 | 1.069 | 0.791 |
| THW_f (s) | 0.816 | 0.891 | 0.566 | 0.589 | 0.770 |
| THW_s (s) | 0.237 | 0.604 | 0.128 | 0.119 | 0.128 |
| $TTCi_d$ (s ⁻¹) | 0.127 | 0.081 | 0.092 | 0.085 | 0.125 |
| $TTCi_f$ (s ⁻¹) | -0.094 | -0.065 | -0.077 | -0.067 | -0.104 |

Driving style indicators computed from each driver during simulated carfollowing scenario. The lead vehicle velocity is the velocity profile of the HWFET driving cycle.

TABLE III DERIVED DRIVING STYLE INDICATORS FOR PARTICIPANTS

| Indicator | Driver1 | СНМ | GM | TMP | AL | OVM | NN |
|---|---------|-------|-------|-------|-------|-----|-------|
| $a_p \text{ (m/s}^2\text{)}$ | 0.549 | 0.397 | 0.346 | 0.481 | 0.437 | - | 1.036 |
| $b_p (\mathrm{m/s^2})$ | 1.712 | 0.267 | 0.138 | 0.541 | 0.762 | - | 1.064 |
| THW_p (s) | 1.211 | 3.424 | 3.094 | 1.198 | 1.264 | - | 1.323 |
| THW_f (s) | 0.361 | 0.313 | 0.120 | 0.278 | 0.574 | - | 0.877 |
| THW_s (s) | 0.349 | 0.665 | 0.677 | 0.214 | 0.344 | - | 0.457 |
| $TTCi_d$ (s ⁻¹) | 0.102 | 0.063 | 0.071 | 0.057 | 0.167 | - | 0.119 |
| $TTCi_f$ (s ⁻¹) | 0.078 | 0.093 | 0.068 | 0.037 | 0.047 | - | 0.062 |
| $\frac{1}{n} \sum \left \frac{I_{dr} - I_m}{I_{dr}} \right $ | | 0.650 | 0.699 | 0.343 | 0.350 | - | 0.496 |

second most aggressive in preferred deceleration. Driver 1 preferred the most dangerous approaching level at $0.127 \, \mathrm{s}^{-1}$. Driver 2 had the longest headway at 3.197 seconds while Driver 5 was following dangerously close at 0.791 seconds.

Control model parameters were estimated by least squares fitting which follows the form:

$$x = \left(A^T A\right)^{-1} A^T a^f \tag{21}$$

where x is the column vector of model gains (c_n) , A is a matrix containing all the model states for the given model, such as v^l and Δd , and a^f is a vector containing each acceleration value from the driver.

After the model construction, each control model was simulated over the EUDC drive cycle for highway speeds (+56 km/h) and indicators were extracted using the same process as with human driver data. To compare and evaluate style indicator reproduction we assume each indicator is of equal weight and take the mean of the absolute relative error between indicators of the driver and driver model given by the formula

$$\frac{1}{n} \sum \left| \frac{I_{dr} - I_m}{I_{dr}} \right| \tag{22}$$

where I_{dr} and I_m represent the indicator for the driver and model and n is the number of indicators. The results of this method are summarized in the Table III through Table VI. At least one model per driver failed to perform the steady following driving task,

TABLE IV
DERIVED DRIVING STYLE INDICATORS FOR PARTICIPANTS

| Indicator | Driver2 | СНМ | GM | TMP | AL | OVM | NN |
|---|---------|-------|-------|-------|-------|-----|----|
| $a_p \text{ (m/s}^2\text{)}$ | 0.622 | 0.416 | 0.382 | 0.435 | 0.364 | - | - |
| $b_p (\mathrm{m/s^2})$ | 1.643 | 0.201 | 0.261 | 0.326 | 0.390 | - | - |
| THW_p (s) | 2.570 | - | - | 3.566 | 3.812 | - | - |
| THW_f (s) | 0.693 | - | - | 0.000 | 0.000 | - | - |
| THW_s (s) | 0.757 | - | - | 0.220 | 0.464 | - | - |
| $TTCi_d$ (s ⁻¹) | 0.102 | 0.020 | 0.023 | 0.015 | 0.017 | - | - |
| $TTCi_f$ (s ⁻¹) | 0.045 | 0.023 | 0.020 | 0.017 | 0.025 | - | - |
| $\frac{1}{n} \sum \left \frac{I_{dr} - I_m}{I_{dr}} \right $ | | - | - | 0.669 | 0.619 | - | - |

TABLE V
DERIVED DRIVING STYLE INDICATORS FOR PARTICIPANTS

| Indicator | Driver3 | CHM | GM | TMP | AL | OVM | NN |
|---|---------|-------|-------|-------|-------|-----|-------|
| - (m /o²) | 1.337 | 1.082 | 1.058 | 1.087 | 1.073 | | 0.726 |
| $a_p (\text{m/s}^2)$ | 1.337 | 1.082 | 1.058 | 1.087 | 1.073 | - | 0.726 |
| $b_p \; (\mathrm{m/s^2})$ | 2.250 | 0.352 | 0.452 | 0.410 | 0.422 | - | 1.008 |
| THW_p (s) | 1.353 | - | - | - | - | - | 1.082 |
| THW_f (s) | 0.420 | - | - | - | - | - | 0.518 |
| THW_{s} (s) | 0.342 | - | - | - | - | - | 0.195 |
| $TTCi_d~(\mathrm{s}^{\text{-}1})$ | 0.083 | 0.026 | 0.045 | 0.028 | 0.020 | - | 0.040 |
| $TTCi_f~(\mathrm{s}^{\text{-}1})$ | 0.061 | 0.148 | 0.148 | 0.041 | 0.043 | - | 0.026 |
| $\frac{1}{n} \sum \left \frac{I_{dr} - I_m}{I_{dr}} \right $ | | - | - | - | - | - | 0.424 |

TABLE VI
DERIVED DRIVING STYLE INDICATORS FOR PARTICIPANTS

| Indicator | Driver4 | CHM | GM | TMP | AL | OVM | NN |
|---|---------|-------|-------|-------|-------|-------|----|
| $a_p (\text{m/s}^2)$ | 0.437 | 0.461 | 0.412 | 0.496 | 0.455 | 1.065 | - |
| $b_p (\mathrm{m/s^2})$ | 1.628 | 0.403 | 0.655 | 0.465 | 0.504 | 1.619 | - |
| THW_p (s) | 1.030 | 1.871 | 2.352 | 0.763 | 0.872 | 1.161 | - |
| THW_f (s) | 0.355 | 0.000 | 0.577 | 0.202 | 0.207 | 0.416 | - |
| THW_s (s) | 0.206 | 0.067 | 0.562 | 0.056 | 0.096 | 0.423 | - |
| $TTCi_d$ (s ⁻¹) | 0.062 | 0.044 | 0.056 | 0.028 | 0.035 | 0.254 | - |
| $TTCi_f$ (s ⁻¹) | 0.050 | 0.054 | 0.049 | 0.025 | 0.038 | 0.296 | - |
| $\frac{1}{n} \sum \left \frac{I_{dr} - I_m}{I_{dr}} \right $ | | 0.522 | 0.628 | 0.475 | 0.358 | 1.543 | - |

denoted by (-). This may be due to poor parameter fitting or the inability to keep a minimum distance. The models that were able to replicate driving style of Driver's 1 through 5 are TMP, AL, NN, AL, and AL, respectively.

The performance of one model for all drivers was compared to our multi-model approach by calculating the mean absolute relative error for indicators of all drivers for which the model does not fail. For example, CHM is a viable choice for three of the drivers so the mean absolute relative error is calculated using all the indicators from each viable driver with $n=21\ (7)$ indicators times three drivers). Fig. 8 shows the results of this comparison with our multi-model (MM) approach having the

TABLE VII
DERIVED DRIVING STYLE INDICATORS FOR PARTICIPANTS

| Indicator | Driver5 | СНМ | GM | TMP | AL | OVM | NN |
|---|---------|-------|-------|-------|-------|-----|-------|
| $a_p \text{ (m/s}^2\text{)}$ | 0.329 | 0.466 | 0.421 | 0.481 | 0.441 | - | 0.625 |
| $b_p (\mathrm{m/s^2})$ | 2.425 | 0.500 | 0.979 | 0.716 | 0.947 | - | 1.521 |
| THW_p (s) | 0.673 | 1.276 | 1.726 | 0.501 | 0.642 | - | 0.708 |
| THW_f (s) | 0.147 | 0.000 | 0.594 | 0.137 | 0.254 | - | 0.284 |
| THW_s (s) | 0.136 | 0.093 | 0.617 | 0.061 | 0.138 | - | 0.316 |
| $TTCi_d$ (s ⁻¹) | 0.097 | 0.064 | 0.104 | 0.032 | 0.142 | - | 0.109 |
| $TTCi_f$ (s ⁻¹) | 0.056 | 0.072 | 0.062 | 0.044 | 0.042 | - | 0.069 |
| $\frac{1}{n} \sum \left \frac{I_{dr} - I_m}{I_{dr}} \right $ | | 0.577 | 1.311 | 0.419 | 0.351 | - | 0.562 |

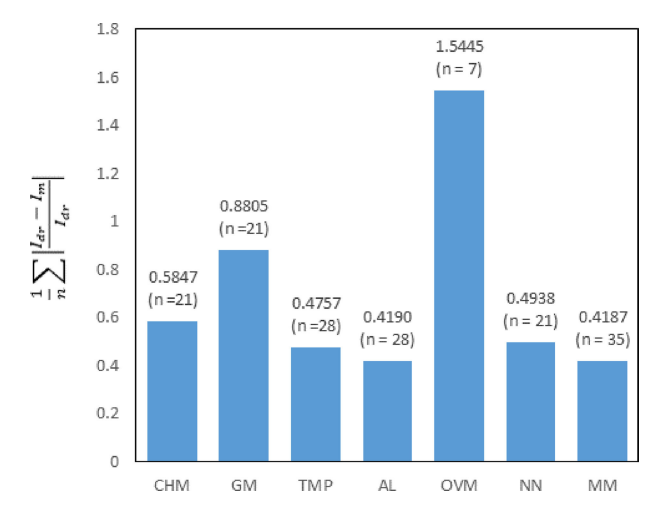


Fig. 8. Driver model performance. Multi-model (MM) approach is to the far right.

TABLE VIII SUCCESS/FAILURE RATE

| СНМ | GM | TMP | AL | OVM | NN | MM |
|-----|-----|-----|-----|-----|-----|-----|
| 3/2 | 3/2 | 4/1 | 4/1 | 1/4 | 3/2 | 5/0 |

least mean absolute relative error of 0.4187 (n=35) followed by AL at 0.4190 (n=28), TMP at 0.4757 (n=28), NN at 0.4938 (n=21), CHM at 0.5847 (n=21), GM at 0.8805 (n=21), and OVM at 1.5445 (n=7). Table VIII shows the number of drivers for which the models were successful at performing the steady following task and the number that failed. While most models did not fail for most of our drivers, our multi-model approach was the only that never fails in addition to having the highest accuracy in terms of style replication.

Next, we utilized the HFWET cycle once more to evaluate the ability of our MPC to track desired velocity while staying within our imposed constraints. Without loss of generality, we use the best model for Driver 1 as an example. Acceleration, velocity, and inter-vehicle distance are shown in Fig. 10. The driver model in this case was shown to become unstable at the end of the cycle, when the lead vehicle comes to a stop. This would

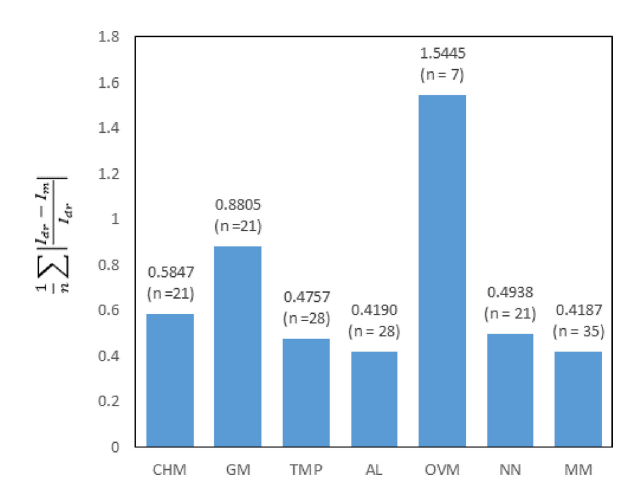


Fig. 9. Acceleration, velocity, and following distance for Driver 1 TMP model simulated over HWFET cycle.

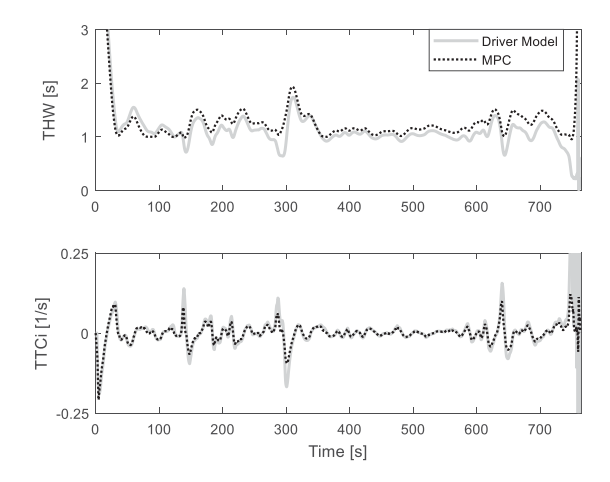


Fig. 10. THW and TTCi for Driver 1 TMP model for the simulated HWFET cycle.

result in the vehicle violently accelerating and braking without further control measures in place. The middle plot shows our MPC tracks the desired velocity, hence acceleration was also closely followed (shown in the upper plot), throughout the cycle but deviated and came to a stop at near the end of the cycle. This phenomenon occurred due to the constraint on minimum distance which is shown at the end of the lower plot, following distance. This constraint naturally improved velocity and acceleration by forcing it to zero when the vehicle was approaching the stopped lead vehicle. However, performance of velocity and acceleration throughout the entire cycle was not necessarily improved, nor was it intended.

The following distance increased over the majority of the cycle due the constraint on THW. The upper plot illustrates that our controller also followed desired acceleration but braked slightly harder to ensure minimum THW was not exceeded. The upper plot of Fig. 9 further proves the MPC did not allow THW below the threshold. THW for the simulation can be seen to not cross below 1 second in Fig. 10. TTCi is also shown in the lower plot, however, the driver only exceeded the limitations at the end of the cycle while the MPC did not.

VII. CONCLUSIONS

We presented a driver data based structure for driver style estimation, model selection via driving style indicator replication, and desired trajectory execution using MPC. Our proposed framework was applied and verified by driver style indicator extraction from data collected through a simulated highway carfollowing scenario. Utilizing the same data, a neural network was implemented and multiple models were constructed using least-squares regression to fit existing model parameters. The models were simulated using a separate highway driving cycle and driving style indicators were compared to that of the driver over the same driving cycle. The "best" model was selected based on the model's ability to reproduce the driver's style, rather than mimicking driver response directly. The "best" model was chosen to produce a reference velocity for our MPC and safety constraints were added to ensure potentially dangerous states did not occur.

Our data-driven approach illustrated, through simulation, driver style can be more closely replicated by one model better than others and is dependent on the individual driver. We showed MPC can accurately replicate the reference velocity generated from the driver model while guaranteeing safe operation of the vehicle during highway speeds and stopping. Our results showed MPC was able to handle situations where the driver model alone failed.

It is worth mentioning that we take the means of the indicators without any filtering because we would like to take all possible driver behaviors into consideration. For instance, without a further investigation, it is difficult to decide whether some high accelerations/decelerations are intentional or misoperations. In this work, as a first step, we consider the mean of all indicator data. As a further extension of the work in the future, we will investigate the context-dependent means to refine the means in different situations, e.g., situations for high maximum accelerations and situations for moderate maximum accelerations. With this investigation, we expect to better discover and represent the driving behaviors of human drivers. In addition, we will also extend our focus to lateral control such as lane keeping and lane switching. We have shown that MPC can appropriately handle some situations which the driver model cannot and would like to apply this knowledge to the full range of autonomous vehicle control functions.

REFERENCES

- [1] R. E. Chandler, R. Herman, and E. W. Montroll, "Traffic dynamics: Studies in car following," *Oper. Res.*, vol. 6, no. 2, pp. 165–184, 1958.
- [2] J. Bengtsson, Adaptive Cruise Control and Driver Modeling. Lund, Sweden: Lund Inst. Technol., 2001.
- [3] Vehicle Technology Survey, Amer. Autom. Assoc., Heathrow, FL, USA, 2016.
- [4] B. Schoettle and M. Sivak, "A survey of public opinion about connected vehicles in the U.S., the U.K., and Australia," in *Proc. 2014 Int. Conf. Connected Veh. Expo.*, 2014, pp. 687–692.
- Connected Veh. Expo., 2014, pp. 687–692.
 [5] T. Al-Shihabi and R. Mourant, "Toward more realistic driving behavior models for autonomous vehicles in driving simulators," *Transp. Res. Res. Board*, vol. 1843, no. 3, pp. 41–49, 2003.
- [6] T. Al-Shaihabi and R. R. Mourant, "A framework for modeling humanlike driving behaviors for autonomous vehicles in driving simulators," in *Proc. 5th Int. Conf. Auton. Agents*, 2001, pp. 286–291.

- [7] V. Vaitkus, P. Lengvenis, and G. Žylius, "Driving style classification using long-term accelerometer information," in *Proc. 2014 19th Int. Conf. Methods Model. Autom. Robot.*, 2014, pp. 641–644.
- [8] M. Bojarski et al., "End to end learning for self-driving cars," CoRR, 2016, arXiv:1604.07316.
- [9] M. Kuderer, S. Gulati, and W. Burgard, "Learning driving styles for autonomous vehicles from demonstration," in *Proc. IEEE Int. Conf. Robot. Autom.*, 2015, pp. 2641–2646.
- [10] C. MacAdam, Z. Bareket, P. Fancher, and R. Ervin, "Using neural networks to identify driving style and headway control behavior of drivers," *Veh. Syst. Dyn.*, vol. 29, no. sup1, pp. 143–160, 1998.
- [11] L. Chong, M. M. Abbas, A. Medina Flintsch, and B. Higgs, "A rule-based neural network approach to model driver naturalistic behavior in traffic," *Transp. Res. Part C Emerg. Technol.*, vol. 32, pp. 207–223, 2013.
- [12] S. Lefèvre, A. Carvalho, and F. Borrelli, "A learning-based framework for velocity control in autonomous driving," *IEEE Trans. Autom. Sci. Eng.*, vol. 13, no. 1, pp. 32—42, Jan. 2016.
- [13] H. Christopher Frey, N. M. Rouphail, and H. Zhai, "Speed- and facility-specific emission estimates for on-road light-duty vehicles on the basis of real-world speed profiles," *Transp. Res. Rec.*, vol. 1987, pp. 128–137, 2006
- [14] M. Brackstone and M. McDonald, "Car-following: A historical review," Transp. Res. Part F Traffic Psychol. Behav., vol. 2, no. 4, pp. 181–196, 1999.
- [15] M. Treiber and A. Kesting, "Microscopic calibration and validation of carfollowing models—A systematic approach," *Procedia, Soc. Behav. Sci.*, vol. 80, pp. 922–939, 2014.
- [16] M. Lu, J. Wang, and K. Li, "Characterisation of longitudinal driving behaviour using measurable parameters," *Transp. Res. Board*, vol. 154, pp. 1–20, 2010.
- [17] V. L. Bageshwar, W. L. Garrard, and R. Rajamani, "Model predictive control of transitional maneuvers for adaptive cruise control vehicles," *IEEE Trans. Veh. Technol.*, vol. 53, no. 5, pp. 1573–1585, Sep. 2004.
- [18] A. Carvalho, Y. Gao, S. Lefevre, and F. Borrelli, "Stochastic predictive control of autonomous vehicles in uncertain environments," in *Proc. 12th Int. Symp. Adv. Veh. Control*, 2014, pp. 712–719.
- [19] S. Lefevre, A. Carvalho, and F. Borrelli, "Autonomous car following: A learning-based approach," in *Proc. IEEE Intell. Veh. Symp.*, 2015, pp. 920– 026.
- [20] A. Carvalho, A. Williams, S. Lefèvre, and F. Borrelli, "Autonomous cruise control with cut-in target vehicle detection," *Adv. Vehicle Control* AVEC'16, pp. 93–98, 2016.
- [21] S. Li, K. Li, R. Rajamani, and J. Wang, "Model predictive multi-objective vehicular adaptive cruise control," *IEEE Trans. Control Syst. Technol.*, vol. 19, no. 3, pp. 556–566, May 2011.
- [22] J.-H. Wang and M. Song, "Assessing drivers' tailgating behavior and the effect of advisory signs in mitigating tailgating," in *Proc. 6th Int. Driving Symp. Human Factors Driver Assessment Train. Veh. Des.*, 2011, pp. 583–589.
- [23] Traffic Safety Facts 2015, National Highway Traffic Safety Administration, Washington, DC, USA, DOT HS 812 384, 2016.
- [24] P. G. Michael, F. C. Leeming, and W. O. Dwyer, "Headway on urban streets: Observational data and an intervention to decrease tailgating," *Transp. Res. Part F Traffic Psychol. Behav.*, vol. 3, no. 2, pp. 55–64, 2000.
- [25] S. Hirst and R. Graham, "The format and presentation of collision warnings," in *Ergonomics and Safety of Intelligent Driver Interfaces*. Boca Raton, FL, USA: CRC Press, 1997, pp. 203–219.
- [26] R. Van der horst and J. Hogema, "Times to collision and collision avoidance systems," in *Proc. 6th ICTCT Workshop*, 1993, pp. 129–143.
- [27] K. Vogel, "A comparison of headway and time to collision as safety indicators," *Accident Anal. Prev.*, vol. 35, no. 3, pp. 427–433, 2003.
- [28] D. C. Gazis, R. Herman, and R. W. Rothery, "Nonlinear follow-the-leader models of traffic flow," *Oper. Res.*, vol. 9, no. 4, pp. 545–567, 1961.
- [29] C. M. J. Tampere, "Human-kinetic multiclass traffic flow theory and modelling with application to advanced driver assistance systems in congestion," doctoral thesis, Faculty Civil Eng. Geosci., Transportation and Planning Section, Delft Univ. Technol., Delft, Netherlands, 2004.
- [30] P. S. Addison and D. J. Low, "A novel nonlinear car-following model," *Chaos*, vol. 8, no. 1998, pp. 791–799, 1998.
- [31] Y. S. M Bando, K Hasebe, A. Nakayama, and A. Shibata, "Dynamical model of traffic congestion and numerical simulation," *Phys. Rev. E, Statist. Phys. Plasmas Fluids Relat. Interdiscip. Topics*, vol. 51, no. 2, pp. 1035– 1042, 1995.

- [32] C. Miyajima et al., "Driver modeling based on driving behavior and its evaluation in driver identification," Proc. IEEE, vol. 95, no. 2, pp. 427–437, Feb. 2007.
- [33] M. Ali, F. Al Machot, A. H. Mosa, and K. Kyamakya, "CNN based subject-independent driver emotion recognition system involving physiological signals for ADAS BT," in *Advanced Microsystems for Automotive Applications 2016: Smart Systems for the Automobile of the Future*, T. Schulze, B. Müller, and G. Meyer, Eds. Berlin, Germany: Springer Int. Publishing, 2016, pp. 125–138.
- [34] Y. Lin, P. Tang, W. J. Zhang, and Q. Yu, "Artificial neural network modelling of driver handling behaviour in a driver \pm vehicle \pm environment system," *Int. J. Veh. Des.*, vol. 37, no. 1, pp. 1–22, 2004.
- [35] D. J. C. MacKay, "Bayesian interpolation," *Neural Comput.*, vol. 4, no. 3, pp. 415–447, 1992.
- [36] F. D. Foresee and M. T. Hagan, "Gauss-Newton approximation to Bayesian learning," in *Proc. 1997 Int. Conf. Neural Netw.*, vol. 3, 1997, pp. 1930– 1935.
- [37] S. Lefevre, A. Carvalho, and F. Borrelli, "Autonomous car following: A learning-based approach," in *Proc. IEEE Intell. Veh. Symp.*, 2015, pp. 920– 926
- [38] T. Hirata, T. Yai, and T. Takagawa, "Development of the driving simulation system MOVIC-T4 and its validation using field driving data," *Tsinghua Sci. Technol.*, vol. 12, no. 2, pp. 141–150, 2007.
- [39] G. H. Bham, M. C. Leu, M. Vallati, and D. R. Mathur, "Driving simulator validation of driver behavior with limited safe vantage points for data collection in work zones," J. Safety Res., vol. 49, pp. 53–60, 2014.



Longxiang Guo received the Bachelor's degree from Tsinghua University, Beijing, China, in 2012, and the Master of Engineering degree from the Chinese Academy of Sciences, Shenzhen, China, in 2015. He is currently working toward the Ph.D. degree in automotive engineering at Clemson University International Center for Automotive Research. He is currently involved in research related to autonomous driving and sensing systems.



Andrew Phillip Bolduc received the Bachelor's degree in mechanical engineering from the Georgia Institute of Technology, Atlanta, GA, USA, in 2012, and the Master's degree in automotive engineering from Clemson University International Center for Automotive Research in 2018. His research interests include driver modeling and model predictive control and their application in autonomous driving.



Yunyi Jia (M'10) received his Ph.D. degree from Michigan State University, East Lansing, MI, USA, in 2014. He is currently an assistant professor in the Department of Automotive Engineering at Clemson University International Center for Automotive Research (CU-ICAR). His research focuses on collaborative robotics, autonomous vehicles, and advanced sensing systems. He is a member of the IEEE, ASME and SAE.